ESI – File S1: Modified Gompertz model development

Microalgal and bacterial growth curves are similar, showing an exponential growth phase. Plotting biomass concentration, *X*, as function of time, *t*, results in a growth curve where three different growth phases can be distinguished. These growth phases can be described by the following parameters: (i) the lag time, λ, defined as the *x*-axis intercept of this tangent; (ii) the maximum specific growth rate, μ_{max}, defined as the tangent in the inflection point; and (iii) the highest biomass concentration achieved or upper asymptote, normally occurring when the stationary growth phase is reached, A. To establish the growth model, the Gompertz equation represented in Equation 3 was rewritten to include the above described growth parameters.

The inflection point of the curve was obtained by calculating the second derivative of the function with respect to *t*:

$$\frac{dy}{dt} = ac \cdot exp[-exp(b-ct)] \cdot exp(b-ct) \quad \text{(S1.1)}$$

$$\frac{d^2y}{dt^2} = ac^2 \cdot exp[-exp(b-ct)] \cdot exp(b-ct) \cdot [exp(b-ct)-1] \quad \text{(S1.2)}$$

At the inflection point, $t = t_i$, the second derivative is equal to 0:

$$\frac{d^2y}{dt^2} = 0 \rightarrow b - ct_i = 0 \leftrightarrow t_i = \frac{b}{c} \quad \text{(S1.3)}$$

$$y_i = a \cdot exp[-exp(0)] = a \cdot exp(-1) = \frac{a}{e} \quad \text{(S1.4)}$$

where y_i corresponds to the output value at time $t = t_i$.

Maximum specific growth rate was then determined by calculating the first derivative at the inflection point:

$$\left(\frac{dy}{dt}\right)_{t_i} = \mu_{max} y_i \leftrightarrow \frac{ac}{e} = \mu_{max} \frac{a}{e} \leftrightarrow \mu_{max} = c \quad \text{(S1.5)}$$

Knowing the point (t_i, y_i) and the slope, $m = \left(\frac{dy}{dt}\right)_{t_i} = \mu_{max} y_i$, the tangent line through the inflection point can be written as:

$$y = \mu_{max} \frac{a}{e} t + \frac{a}{e}(1 - \mu_{max} t_i) \quad \text{(S1.6)}$$

The lag time, λ, is defined as the *t*-axis intercept of the tangent through the inflection point:

$$0 = \mu_{max} \frac{a}{e} \lambda + \frac{a}{e}(1 - \mu_{max} t_i) \quad \text{(S1.7)}$$

Using Equations S1.3, S1.5 and S1.7, the lag time corresponds to:

$$\lambda = \frac{b - 1}{c} \quad \text{(S1.8)}$$

By substituting the parameters a, b and c from the Gompertz equation, the modified Gompertz model was obtained:

$$X = A \cdot exp\left[- exp\left(\mu_{max}(\lambda - t) + 1\right)\right] \quad \text{(S1.9)}$$

ESI – File S2: Performance indexes of the model fits

The quality of the model fits was evaluated by calculating the following performance indexes:

(i) Root mean squared error ($RMSE$) measures the agreement between data obtained empirically and predicted values. The null value for this performance parameter indicates a perfect fit between predicted and experimental data.

$$RMSE = \sqrt{\frac{\sum (z - \hat{z})^2}{n}} \quad \text{(S2.1)}$$

where z denotes the experimental values, $\hat{z}$ the predicted values by the model and n the data size.

(ii) Standard error of prediction ($\%SEP$) corresponds to standardized $RMSE$. A $\%SEP$ of zero also denotes a perfect fit between predicted and experimental data.

$$\%SEP = \frac{100}{\bar{z}} \sqrt{\frac{\sum (z - \hat{z})^2}{n}} \quad \text{(S2.2)}$$

where $\bar{z}$ denotes the mean of the experimental values.

(iii) Bias factor (B_f) is an objective indicator of model performance, since the perfect fit is determined by a B_f of one.

$$B_f = 10^{\frac{\log \sum \log (\hat{z}/z)}{n}} \quad \text{(S2.3)}$$

(iv) Accuracy factor (A_f) represents the difference between the mean observed values and the predicted ones. An A_f of one also denotes a perfect fit between predicted and experimental data. An increase in this factor results in a low capacity of the model to simulate empirical data.

$$A_f = 10^{\frac{\sum|\log(\hat{z}/z)|}{n}} \quad \text{(S2.4)}$$

ESI – File S3: Growth curves

Growth curves obtained for mono- and co-cultures of *S. salina* and *P. subcapitata* grown under varying phosphate-phosphorus concentrations are shown in Figure 3.1.

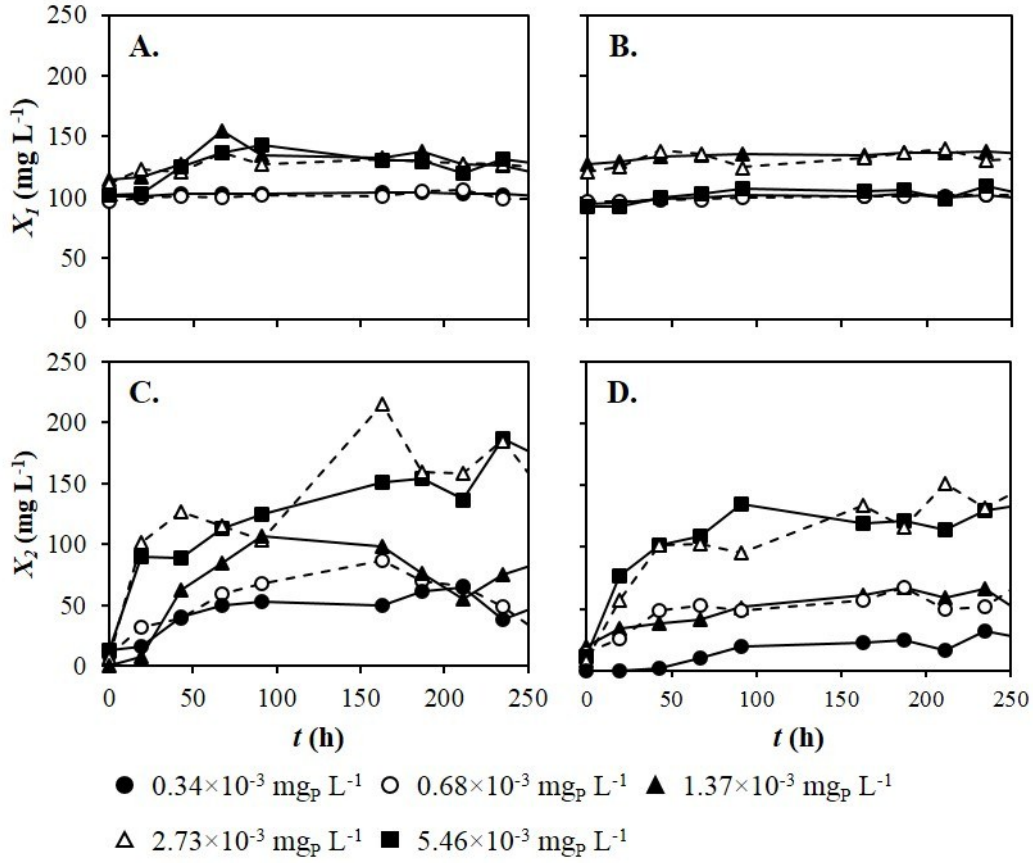

Figure S3.1. Growth curves of mono- and co-cultures of *S. salina* and *P. subcapitata* grown under varying phosphorus concentrations: A. *S. salina* grown in mono-cultures; B. *S. salina* grown in co-cultures; C. *P. subcapitata* grown in mono-cultures; D. *P. subcapitata* grown in co-cultures.

ESI – File S4: GC-MS and 1D-NMR analysis

The compounds identified by GC-MS with a percentage of similarity with NIST library higher than 80% are listed in Table S4.1. The organic acids used in antimicrobial studies are highlighted in bold.

Table S4.1. Compounds identified in co-cultures medium of *S. salina* and *P. subcapitata* by gas chromatography coupled with electron ionization mass spectrometry (GC-MS)

	Compound	**Molecular formula***	**Molecular weight***	**% Similarity****
1	2,2,2-Trifluoroacetamide	$C_8H_{18}F_3NOSi_2$	257	81
2	Octamethyltrisiloxane	$C_8H_{24}O_2Si_3$	236	91
3	*N-tert*-Butylmethylamine	$C_7H_{21}NSi_2$	175	91
4	Piperidine	$C_8H_{19}NSi$	157	87
5	**2-Hydroxypropanoic acid**	**$C_9H_{22}O_3Si_2$**	**234**	**91**
6	Alanine	$C_9H_{23}NO_2Si_2$	233	90
7	Glycine	$C_8H_{21}NO_2Si_2$	219	80
8	Dodecamethylpentasiloxane	$C_{12}H_{36}O_4Si_5$	384	90
9	L-Valine	$C_{11}H_{27}NO_2Si_2$	261	86
10	Urea	$C_7H_{20}N_2OSi_2$	204	95
11	Aminoethanol	$C_{11}H_{31}NOSi_3$	277	99
12	Glycerol	$C_{12}H_{32}O_3Si_3$	308	91
13	L-Isoleucine	$C_{12}H_{29}NO_2Si_2$	275	90
14	L-Proline	$C_{11}H_{25}NO_2Si_2$	259	91
15	Glycine,	$C_{11}H_{29}NO_2Si_3$	291	83
16	**Butanedioic acid**	**$C_{10}H_{22}O_4Si_2$**	**262**	**87**
17	Serine	$C_{12}H_{31}NO_3Si_3$	321	91

18	L-threonine	$C_{13}H_{33}NO_3Si_3$	335	91
19	Butane	$C_{16}H_{42}O_4Si_4$	410	86
20	L-Aspartic acid	$C_{13}H_{31}NO_4Si_3$	349	96

* Characterized as silane derivatives

** Percentage of similarity with NIST library.

Table S4.1. (continued)

Compound		Molecular formula*	Molecular weight*	% Similarity**
21	**4-Aminobutanoic acid**	**$C_{13}H_{33}NO_2Si_3$**	**319**	**86**
22	**2,3,4-Trihydroxybutanoic acid**	**$C_{16}H_{40}O_5Si_4$**	**424**	**95**
23	Ornithine	$C_{14}H_{36}N_2O_2Si_3$	348	99
24	Glutamine	$C_{14}H_{33}NO_4Si_3$	363	99
25	Phenylalanine	$C_{15}H_{27}NO_2Si_2$	309	91
26	Arabinopyranose	$C_{17}H_{42}O_5Si_4$	438	94
27	Arabinose	$C_{17}H_{42}O_5Si_4$	438	94
28	L-Asparagine,	$C_{13}H_{32}N_2O_3Si_3$	348	99
29	l-(-)-Arabitol	$C_{20}H_{52}O_5Si_5$	512	93
30	D-Galactose,	$C_{21}H_{52}O_6Si_5$	540	83
31	α-D-Mannopyranose	$C_{21}H_{52}O_6Si_5$	540	93
32	Talose	$C_{21}H_{52}O_6Si_5$	540	94
33	L-Tyrosine	$C_{18}H_{35}NO_3Si_3$	397	91
34	L-Lysine	$C_{18}H_{46}N_2O_2Si_4$	434	94
35	D-Glucose	$C_{21}H_{52}O_6Si_5$	540	94
36	Myo-Inositol	$C_{24}H_{60}O_6Si_6$	612	99
37	β-D-Galactofuranose	$C_{21}H_{52}O_6Si_5$	540	80
38	D-Mannopyranose	$C_{21}H_{52}O_6Si_5$	540	80
39	β-D-Galactofuranose	$C_{21}H_{52}O_6Si_5$	540	91
40	α-D-Glucopyranoside	$C_{36}H_{86}O_{11}Si_8$	918	94

* Characterized as silane derivatives

** Percentage of similarity with NIST library.

.

In Figure S4.1 the 1D-NMR spectrum of the co-cultures of *S. salina* and *P. subcapitata* medium where several organic compounds (amino acids, organic acids and alcohols) were identified is shown.

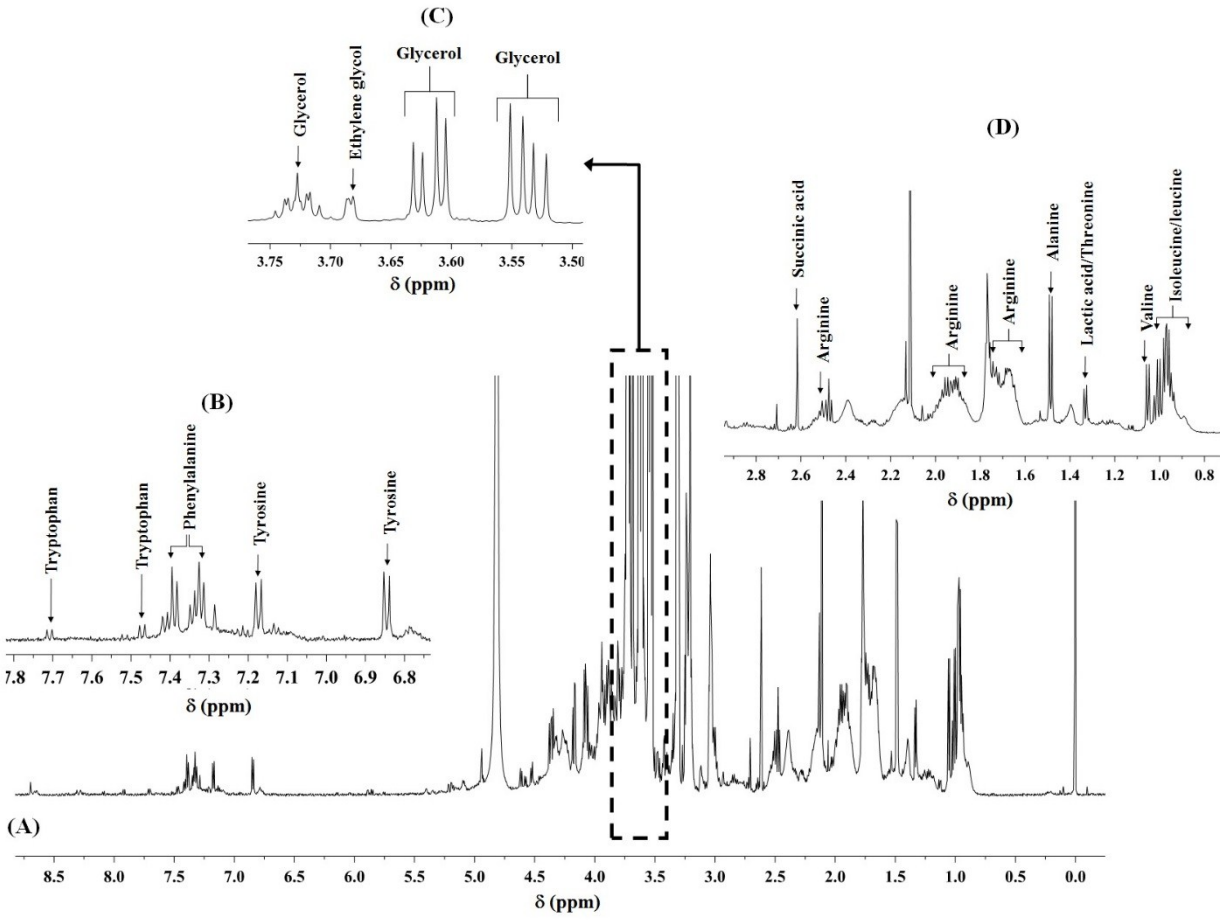

Figure S4.1. 1H NMR spectrum (A) of the co-cultures medium of *Synechocystis salina* and *Pseudokirchneriella subcapitata* showing expanded spectrum: (B) from 6.8 to 7.8 ppm; (C) from 3.50 to 3.75ppm; and (D) from 0.8 to 2.8 ppm.

ESI – File S5: Disc diffusion method

Figure S5.1 shows the results of the disc diffusion method applied to evaluate the potential of 2-hydroxypropanoic acid (5), 1,4-butanedioic acid (16), 4-aminobutanoic acid (21) and 2,3,4-trihydroxybutanoic acid (22) against *S. salina* and *P. subcapitata*. From this figure, it is possible to see that 2-hydroxypropanoic acid presented an inhibitory effect towards *S. salina*, but not towards *P. subcapitata*. The other studied compounds have not shown activity against the studied microorganisms.

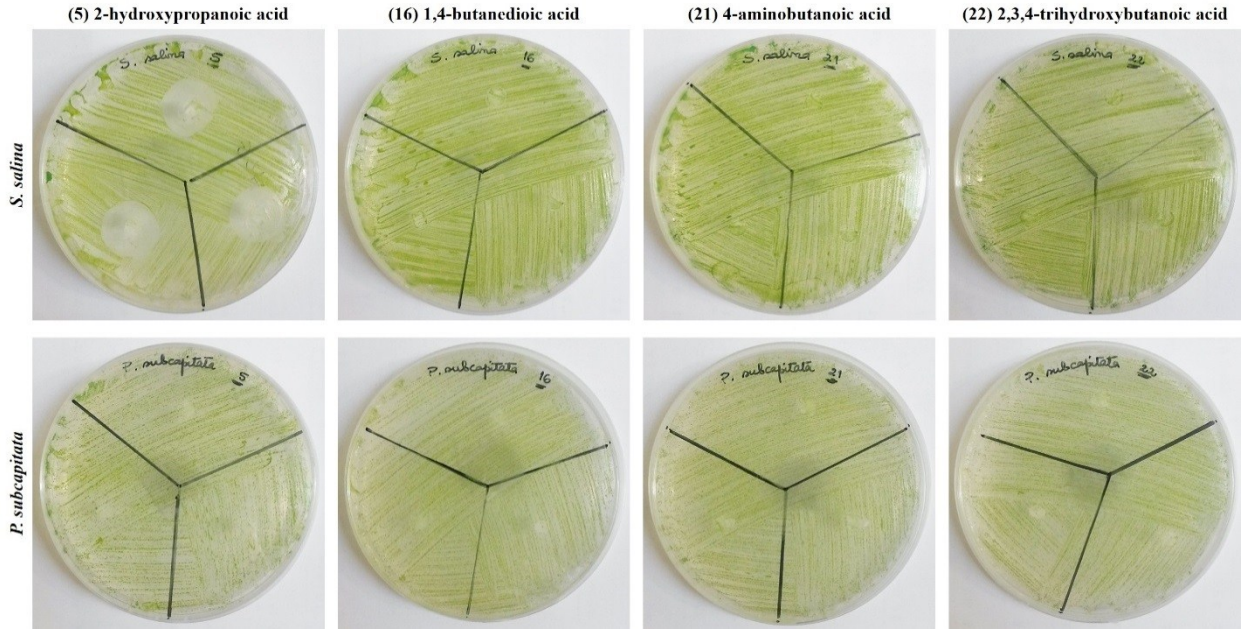

Figure S5.1. Photographs of the Petri dishes after application of the disc diffusion method to evaluate the antimicrobial activity of 2-hydroxypropanoic acid (5), 1,4-butanedioic acid (16), 4-aminobutanoic acid (21) and 2,3,4-trihydroxybutanoic acid (22) against *Synechocystis salina* and *Pseudokirchneriella subcapitata*.